13th National Conference on Mechanisms and Machines (NaCoMM07),
IISc, Bangalore, India. December 12-13, 2007

NaCoMM-2007-102

Constrained Motion Interpolation for Planar 6R Closed Chains

Anurag Purwar[*], Zhe Jin, Q. J. Ge

Department of Mechanical Engineering, Stony Brook University, New York, USA

[*] Corresponding author (email: anurag.purwar@stonybrook.edu)

Abstract

This paper deals with the motion interpolation of an object that satisfies the kinematic constraints imposed by planar 6R closed chains. The paper brings together the well-known kinematics of planar 6R closed chains and the freeform rational motions to synthesize the constrained piecewise rational motions in the Cartesian space. The methodology adopted in this paper is based on transforming the kinematic constraints of planar 6R closed chains into geometric constraints and the problem of designing C^2 continuous rational motions is treated as designing smooth splines in the space of planar displacement matrix parameters. In contrast to another approach of designing smooth splines in the space of planar quaternions, this approach has the advantage of being direct and yields lower degree motions. The results have application in task specification in mechanism synthesis and Cartesian motion planning in robotics.

Keywords: Rational Motions, Constrained Motion Interpolation, Planar Kinematic closed chains

1 Introduction

This paper studies the problem of synthesizing smooth piecewise rational interpolating motion of planar 6R closed chains under kinematic constraints. Given a set of displacements of the coupler of a planar 6R closed chain, the objective is to synthesize a C^2 continuous piecewise rational motion that interpolates the given displacements and satisfies the kinematic constraints of a planar 6R closed chain. Kinematic constraints under consideration are rigid body constraints and workspace related constraints that limit the position of the links of planar closed chains in the Cartesian space. The rationale behind the choice of rational motions stems from the fact that the trajectories of an object undergoing rational motions are rational curves and surfaces, thereby making them suitable for existing Non-uniform Rational B-spline (NURBS) based CAD/CAM system.

The work reported in this paper rests on the well-known idea of application of geometry based CAGD algorithms (Farin [1], and Piegl and Tiller [2]) in the image space of displacements (Ravani and Roth [3]) for giving rise to freeform rational motions. For details on rational motion, see Ge and Ravani [4, 5], Jüttler and Wagner [6], Wagner [7],

Röschel [8], and Purwar and Ge [9]. However, this study differs from the aforementioned work in that our focus is on the rational motions under *kinematic constraints* and we synthesize such motions directly using the elements of the homogeneous form of displacement matrix. Although the work by Horsch and Jüttler [10] and Wagner and Ravani [11] on direct application of rational motions to Cartesian motion planning of robots seems related, they have not dealt with rational motions under kinematic constraints. Very recently, for the first time, Jin and Ge [12, 13] studied the problem of motion interpolation under kinematic constraints for planar 2R, 3R open chains, as well as 6R closed chains, while Purwar et al. [14, 15] studied the same problem for spherical 2R, 3R robot arms and 6R closed chains. Their approach involved using quaternions to represent planar and spherical displacements (see Bottema and Roth [16] and McCarthy [17] for quaternion representation of displacements). The kinematic constraints are transformed into geometric constraints and the problem of synthesizing smooth piecewise rational motions is converted into that of designing smooth piecewise rational curves in the space of quaternions under the geometric constraints. Pursuant to that work, Jin and Ge [18] investigated directly employing the elements of the matrix of a planar displacement for motion interpolation of both revolute and prismatic jointed open planar chains. This paper extends that work to planar 6R closed chains and shows that the problem of motion interpolation under the kinematic constraints of a planar 6R closed chain can be effectively solved using an iterative algorithm. It is also shown that the same algorithm can be used for motion interpolation of planar 4R and 5R closed chains under kinematic constraints.

Advantages of directly using the elements of displacement matrix (as opposed to quaternions) for motion interpolation are that the interpolation process is straightforward and the resulting motion is of lower degree; e.g., cubic interpolation of planar quaternions produces a motion of degree six, while that of the elements of displacement matrices produces a motion of degree three only. We note that the degree mentioned here pertains to the motion interpolation parameter, usually associated with time.

In this paper, the kinematic constraints of the closed chain are formulated in terms of the elements of the matrix, thus giving rise to the constraint manifold in the parameter space of the matrix elements. In the space of the matrix elements, this manifold is given by algebraic equations and can be seen

13th National Conference on Mechanisms and Machines (NaCoMM07),
IISc, Bangalore, India. December 12-13, 2007

NaCoMM-2007-102

as describing geometric constraints. Given a series of coupler's positions in Cartesian space, the problem of synthesizing the smooth interpolating rational motion of a planar 6R closed chain is reduced to that of designing a C^2 continuous rational spline constrained to lie on the constraint manifold. To solve this problem, first a free-form C^2 continuous B-spline curve interpolating through the given positions is designed in the parameter space. An iterative algorithm detects the violation of the kinematic constraints by searching for those extreme points of the curve that do not satisfy the geometric constraints. Such extreme points are replaced with new points that satisfy the constraints and the resulting new points are added to the ordered set of the initial positions to be interpolated. An example is given to show how this algorithm produces smooth planar rational spline motions that satisfy the kinematic constraints of a planar 6R closed chain.

The organization of the paper is as follows" Section 2 presents the algebraic form of kinematic constraints in terms of the elements of the displacement matrix of planar closed 4R, 5R, and 6R kinematic chains. Section 3 deals with the problem of constrained motion interpolation in a parametric space defined by the elements of the displacement matrix and presents an algorithm for the problem of rational motion planning for planar 6R closed chains. An example is presented to illustrate the working of the algorithm. Section 5 discusses how the motion interpolation problem can be solved for 4R and 5R closed chains using the same algorithm.

2 Kinematics of Planar Closed Kinematic Chains

This section derives the algebraic relations that characterize the kinematic constraints of various closed planar chains in terms of the displacement matrix elements. However, we first present a planar quaternion based formulation of the kinematics of planar closed chains and then derive the matrix element formulation of constraints. The goal is to present a representation of rational motions that can easily handle the kinematic constraints of the planar chains.

2.1 Planar quaternions

For a planar displacement shown in Figure 1, let d_1, d_2 denote the coordinates of the origin of the moving frame $\mathbf{M}$ in the fixed frame $\mathbf{F}$ and α denote the rotation angle of $\mathbf{M}$ relative to $\mathbf{F}$. Then the planar displacement can be presented by a planar quaternion, $\mathbf{Y} = Y_1\varepsilon\mathbf{i} + Y_2\varepsilon\mathbf{j} + Y_3\mathbf{k} + Y_4$, where $(\mathbf{i}, \mathbf{j}, \mathbf{k}, 1)$ form the quaternion basis and ε is the dual unit with the property $\varepsilon^2 = 0$. The components of the planar quaternion, $\mathbf{Y} = (Y_1, Y_2, Y_3, Y_4)$, are given by McCarthy [17]:

$$Y_1 = \frac{d_1}{2}\cos\frac{\alpha}{2} + \frac{d_2}{2}\sin\frac{\alpha}{2}, \quad Y_2 = -\frac{d_1}{2}\sin\frac{\alpha}{2} + \frac{d_2}{2}\cos\frac{\alpha}{2},$$
$$Y_3 = \sin\frac{\alpha}{2}, \qquad\qquad Y_4 = \cos\frac{\alpha}{2}.$$
$$(1)$$
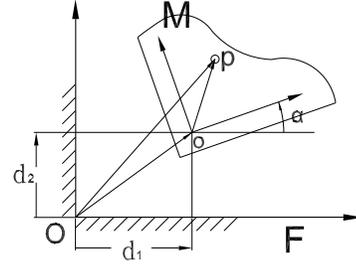
Figure 1: A planar displacement.

In view of (1), we have

$$Y_3^2 + Y_4^2 = 1. \tag{2}$$

The components of a planar quaternion are related to the homogeneous transform of a planar displacement by:

$$[M] = \begin{bmatrix} m_1 & -m_2 & m_3 \\ m_2 & m_1 & m_4 \\ 0 & 0 & 1 \end{bmatrix}, \tag{3}$$

where

$$m_1 = (Y_4^2 - Y_3^2)/(Y_3^2 + Y_4^2), \qquad m_2 = 2Y_3Y_4/(Y_3^2 + Y_4^2),$$
$$m_3 = 2(Y_1Y_4 - Y_2Y_3)/(Y_3^2 + Y_4^2), \quad m_4 = 2(Y_1Y_3 + Y_2Y_4)/(Y_3^2 + Y_4^2).$$
$$(4)$$

It follows that

$$m_1^2 + m_2^2 = 1. \tag{5}$$

This circular constraint (5) ensures that the homogeneous transform $[M]$ represents a rigid-body transformation. This constraint is an inherent property of the planar rigid body displacement matrices.

If $\mathbf{m} = (m_1, m_2, m_3, m_4)$ are rational functions of degree n in parameter u (u being usually associated with time), such that the circular condition (5) is satisfied, then the matrix $[M]$ represents a rational motion of degree n. On the other hand, from Eq. (4) it is clear that choosing planar quaternion $\mathbf{Y} = (Y_1, Y_2, Y_3, Y_4)$ to construct a rational motion would produce a rational motion of degree $2n$. In this paper, we use $\mathbf{m} = (m_1, m_2, m_3, m_4)$ directly to construct a rational motion.

Let $\mathbf{m}_i = (m_{i1}, m_{i2}, m_{i3}, m_{i4})$; $i = 0, ..., n$ be $(n+1)$ vectors of displacement matrix parameters, then the following represents a B-Spline curve in the parameter space:

$$\mathbf{m}(u) = \sum_{i=0}^{n} N_{i,p}(u)\mathbf{m}_i. \tag{6}$$

where $N_{i,p}(u)$ are pth-degree basis functions. A representation for the rational B-Spline motion in the Cartesian space is obtained by substituting $\mathbf{m}(u)$ from Eq. (6) into the homogeneous matrix $[M]$. From Eq. (3), it can be seen that if the B-Spline curve $\mathbf{m}(u)$ is expressed as a polynomial function of degree p, then the matrix $[M]$ represents a rational B-Spline motion of degree p.

13th National Conference on Mechanisms and Machines (NaCoMM07),
IISc, Bangalore, India. December 12-13, 2007

NaCoMM-2007-102
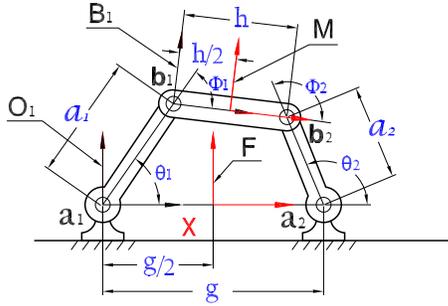
Figure 2: A planar 4R closed chain.

2.2 Planar 4R Closed Chain

A planar 4R closed chain is composed of a pair of planar 2R open chains with their end links rigidly connected; see Fig. 2. This planar 4R closed chain has one degree of freedom so the constraint manifold is a curve, which is the intersection of two constraint surfaces governed by two planar 2R open chains.

Select the fixed frame **F** so that it is at the midpoint between a_1 and a_2, and the moving frame **M** at the midpoint between b_1 and b_2. The position of the moving frame **M** is composed of a translation from **F** to O_1 with a planar quaternion $G_1 = (-g/4, 0, 0, 1)$, a displacement of B_1 relative to O_1 with $Z(\theta_1, \phi_1)$, and another translation from B_1 to **M** with a planar quaternion $H_1 = (h/4, 0, 0, 1)$. Combining all these displacements, we obtain the following transformation from **F** to **M**:

$$Y_1(\theta_1, \phi_1) = G_1 Z(\theta_1, \phi_1) H_1 = [C_1]Z(\theta_1, \phi_1), \quad (7)$$

where the planar quaternions $Z(\theta_1, \phi_1), Y_1(\theta_1, \phi_1)$, and the matrix $[C_1]$ are given in Jin and Ge [12, 13].

Substituting $Y_i; i = 1 \ldots 4$ from Jin and Ge [12, 13] into Eq. (4), we obtain elements of the homogeneous matrix $[M]$, given by m_1:

$$m_1 = \cos(\theta_1 + \phi_1), m_2 = \sin(\theta_1 + \phi_1),$$
$$m_3 = a_1 \cos\theta_1 + (\sigma - \tau)\cos(\theta_1 + \phi_1) - (\sigma + \tau), \quad (8)$$
$$m_4 = a_1 \sin\theta_1 + (\sigma - \tau)\sin(\theta_1 + \phi_1),$$

where,

$$\sigma = (g + h)/4, \quad \tau = (g - h)/4. \quad (9)$$

Similarly the planar quaternion representing the other planar 2R open chain is given by:

$$Y_2(\theta_2, \phi_2) = [C_2]Z(\theta_2, \phi_2), \quad (10)$$

Substituting $Y_i; i = 1 \ldots 4$ from Eq. (10) into Eq. (4), we obtain elements of the homogeneous matrix $[M]$, given by m_2:

$$m_1 = \cos(\theta_2 + \phi_2), m_2 = \sin(\theta_2 + \phi_2),$$
$$m_3 = a_2 \cos\theta_2 + (\tau - \sigma)\cos(\theta_1 + \phi_1) + (\sigma + \tau), \quad (11)$$
$$m_4 = a_2 \sin\theta_2 + (\tau - \sigma)\sin(\theta_1 + \phi_1).$$

The constraint curve for the planar 4R closed chain is the intersection of the constraint surfaces given by (8) and

(11), that is $m_1 = m_2 = m = (m_1, m_2, m_3, m_4)$. The algebraic equations for the kinematic constraints are obtained by eliminating $\theta_i, \phi_i; i = 1, 2$ from Eqs. (8) and (11):

$$m_1^2 + m_2^2 = 1,$$
$$(m_3 - (\sigma - \tau)m_1 + (\sigma + \tau))^2 + (m_4 - (\sigma - \tau)m_2)^2 = a_1^2,$$
$$(m_3 + (\sigma - \tau)m_1 - (\sigma + \tau))^2 + (m_4 + (\sigma - \tau)m_2)^2 = a_2^2.$$
$$(12)$$

In this paper, the constraint equations of the form (12) will be used for rational motion synthesis.

2.3 Planar 5R Closed Chain
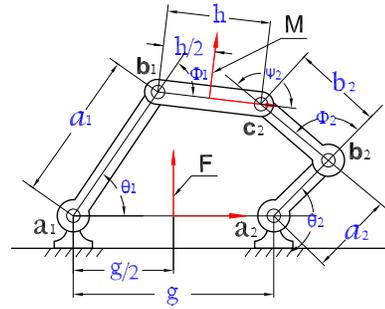
Figure 3: A planar 5R closed chain.

Consider a planar 5R closed chain; see Figure 3. The constraint manifold for this planar 5R closed chain is a portion of the constraint surface of a planar 2R open chain cut by the inner and outer boundaries of the constraint manifold of a planar 3R open chain.

The constraint surface of a planar 2R open chain is given by Eq. (8). The constraint manifold of a planar 3R open chain is given by:

$$Y_2(\theta_2, \phi_2, \psi_2) = [C_2]Z(\theta_2, \phi_2, \psi_2), \quad (13)$$

where $Z(\theta_2, \phi_2, \psi_2), Y_2(\theta_2, \phi_2, \psi_2)$ and $[C_2]$ are given in Jin and Ge [12, 13].

Substituting Y_2 into Eq. (4), we obtain elements of the homogeneous matrix $[M]$:

$$m_1 = \cos(\theta_2 + \phi_2 + \psi_2), m_2 = \sin(\theta_2 + \phi_2 + \psi_2),$$
$$m_3 = a_2 \cos\theta_2 + b_2 \cos(\theta_2 + \phi_2) - (\sigma - \tau)\cos(\theta_2 + \phi_2 + \psi_2)$$
$$\quad + (\sigma + \tau),$$
$$m_4 = a_2 \sin\theta_2 + b_2 \sin(\theta_2 + \phi_2) - (\sigma - \tau)\cos(\theta_2 + \phi_2 + \psi_2).$$
$$(14)$$

Once again, the kinematic constraint equations are obtained by eliminating θ_2, ϕ_2, ψ_2 from Eq. (14). Assembling all the constraint equations:

$$m_1^2 + m_2^2 = 1,$$
$$(m_3 - (\sigma - \tau)m_1 + (\sigma + \tau))^2 + (m_4 - (\sigma - \tau)m_2)^2 = a_1^2,$$
$$(m_3 + (\sigma - \tau)m_1 - (\sigma + \tau))^2 + (m_4 + (\sigma - \tau)m_2)^2 = R_2^2(\phi_2),$$
$$(15)$$

where

$$R_2^2(\phi_2) = a_2^2 + b_2^2 + 2a_2 b_2 \cos(\phi_2),$$
$$|a_2 - b_2| \le R_2(\phi_2) \le (a_2 + b_2). \quad (16)$$

13th National Conference on Mechanisms and Machines (NaCoMM07),
IISc, Bangalore, India. December 12-13, 2007

NaCoMM-2007-102

2.4 Planar 6R Closed Chain
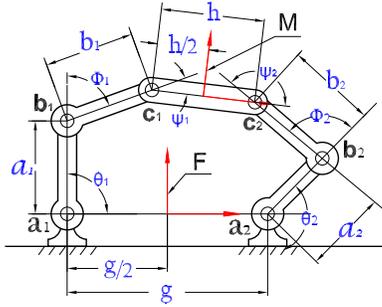
Figure 4: A planar 6R closed chain.

Consider a planar 6R closed chain; see Figure 4. The constraint manifold for this planar 6R closed chain is the intersection of constraint manifolds of two planar 3R open chains. Similar to the case of a planar 5R closed chain, the two constraint manifolds for the 6R chain are given by

$$
\begin{aligned}
\mathbf{Y}_1(\theta_1, \phi_1, \psi_1) &= [C_1]\mathbf{Z}(\theta_1, \phi_1, \psi_1), \qquad (17)\\
\mathbf{Y}_2(\theta_2, \phi_2, \psi_2) &= [C_2]\mathbf{Z}(\theta_2, \phi_2, \psi_2).
\end{aligned}
$$

Following the same procedure as outlined in the previous subsections, the kinematic constraints in terms of the elements of the homogeneous matrix $[M]$ for a planar 6R closed chain are obtained and given by:

$$
\begin{aligned}
m_1^2 + m_2^2 &= 1,\\
(m_3 - (\sigma - \tau)m_1 + (\sigma + \tau))^2 + (m_4 - (\sigma - \tau)m_2)^2 &= R_1^2(\phi_1),\\
(m_3 + (\sigma - \tau)m_1 - (\sigma + \tau))^2 + (m_4 + (\sigma - \tau)m_2)^2 &= R_2^2(\phi_2),
\end{aligned}
$$
(18)

where

$$
\begin{aligned}
R_1^2(\phi_1) &= a_1^2 + b_1^2 + 2a_1b_1\cos(\phi_1),\\
|a_1 - b_1| &\le R_1(\phi_1) \le (a_1 + b_1),
\end{aligned}
$$
(19)

and $R_2(\phi_2)$ is given by Eq. (16).

3 Rational Motions of Planar 6R Closed Chain

In this section, we present an algorithm adopted from Purwar et al. [15] for synthesizing C^2 continuous piecewise rational motions of planar 6R closed chain under the kinematic constraints derived in the previous section.

3.1 C^2 Interpolating Rational Motion for Planar 6R Closed Chain

Given: A set of positions of the coupler link of a planar 6R closed chain in its workspace, the corresponding parameter values $u_i (i = 1 \ldots n)$, lengths of the links given by $a_i, b_i (i = 1, 2)$, and the distance between the two moving pivots and between the two fixed pivots given by h and g, respectively.

Find: A C^2 rational motion of the coupler link that interpolates the given positions at the respective parameter values

subject to the kinematic constraints of the planar 6R closed chain.

In what follows, we first present a sketch of the algorithm:

1. Given positions of the coupler are converted to the elements of the displacement matrix; this gives us a set of element vectors, $\mathbf{m}_i; i = 0 \ldots n$. An initial interpolating C^2 B-spline curve $\mathbf{m}(u)$ is constructed[1] in the space of the elements of the displacement matrix using Eq. (6).

2. The curve $\mathbf{m}(u)$ in the parameter space should satisfy following geometric constraints (rewritten from Eq. (18) and slightly modified from Eq. (5)):

$$(a_1 - b_1)^2 \le F_1(u) \le (a_1 + b_1)^2, \qquad (20)$$

$$(a_2 - b_2)^2 \le F_2(u) \le (a_2 + b_2)^2, \qquad (21)$$

$$(1.0 - \delta)^2 \le F_3(u) \le (1.0 + \delta)^2, \qquad (22)$$

where

$$
\begin{aligned}
F_1(u) &= (m_3(u) - (\sigma - \tau)m_1(u) + (\sigma + \tau))^2 + (m_4(u) - \\
&\quad (\sigma - \tau)m_2(u))^2,\\
F_2(u) &= (m_3(u) + (\sigma - \tau)m_1(u) - (\sigma + \tau))^2 + (m_4(u) + \\
&\quad (\sigma - \tau)m_2(u))^2,
\end{aligned}
$$

and $F_3(u) = m_1^2(u) + m_2^2(u)$. In Eq. (22), δ is a user-defined value that can be chosen as small as desired to approximate the circular constraints. Here, we have modified the form of (5) to an inequality constraint for numerical computation.

Since a C^2 B-spline curve, such as $\mathbf{m}(u)$ has a piecewise cubic Bézier representation, it is easy to evaluate the first order derivative of functions $F_i(u); i = 1, 2, 3$ and verify if the geometric constraints given above are satisfied. The solution of following equations yields the extrema of functions $F_i(u); i = 1, 2, 3$:

$$\frac{dF_1(u)}{du} = 0, \quad \frac{dF_2(u)}{du} = 0, \quad \frac{dF_3(u)}{du} = 0. \qquad (23)$$

If an extremum of any of the functions $F_i(u)$ is outside the corresponding inequality given in Eqs. (20), (21), or (22), the constraints are considered violated. Such a constraint violating extremum (say, at $u = u^*$) is called an extreme point $\mathbf{m}^*$ on the parameter space curve $\mathbf{m}(u)$.

3. If an extreme point is found at $u = u^*$, this point is replaced with a new point $\mathbf{m}(u^*)$ that satisfies the geometric constraints (Eqs. (20), (21), and (22)) and added to the initial set of positions given to be interpolated. A new C^2 B-spline curve is generated that interpolates this new point as well. We also require this new point to be minimally away from the extreme point so as to allow

---

[1]Designing a C^2 B-spline curve is a standard scheme in CAGD (see Farin [1] and Piegl and Tiller [2]).

13th National Conference on Mechanisms and Machines (NaCoMM07),
IISc, Bangalore, India. December 12-13, 2007

NaCoMM-2007-102

the least amount of change in the shape of the previously generated curve. If the new curve satisfies all the constraints, we stop otherwise we repeat the procedure outlined above.

4. The issue of finding a new point that is minimally away from an extreme point can be turned into a normal distance minimization problem in the parameter space. This problem has been effectively solved by Ravani and Roth [19], who gave a general algebraic method for approximate normal distance calculation between the image curve and a given position in the image space. However, our operating space in this paper being a parameter space rather than an image space, a proper metric for this space has to be defined. We now show via a simple derivation that our choice of a metric for the space of the elements of the displacement matrix is directly related to the metric used by Ravani and Roth [19] for planar displacements: Normal distance in the image space of planar displacements is given by $\mathbf{Y}^T\mathbf{Y} = Y_1^2 + Y_2^2 + Y_3^2 + Y_4^2$, where $\mathbf{Y} = (Y_1, Y_2, Y_3, Y_4)$ is a planar quaternion. Using Eqs. (2) and (4), we obtain:

$$m_1^2 + m_2^2 + \frac{1}{4}m_3^2 + \frac{1}{4}m_4^2 = Y_1^2 + Y_2^2 + Y_3^2 + Y_4^2 \quad (24)$$

or, $\quad \mathbf{m}^T[Q]\mathbf{m} = \mathbf{Y}^T\mathbf{Y}$, $\quad$ where $\quad [Q] =$
$\begin{pmatrix} 1 & 0 & 0 & 0 \\ 0 & 1 & 0 & 0 \\ 0 & 0 & 1/4 & 0 \\ 0 & 0 & 0 & 1/4 \end{pmatrix}$ Thus, to calculate normal

distance between two points in the parameter space, expression $\mathbf{m}^T[Q]\mathbf{m}$ should be used.

We note here that the choice of a metric for planar or spatial displacements is a continuing topic of research (see Angeles [20] for the latest on this topic) due to the problem associated with combining translation and rotation in a meaningful way. Our choice of metric in the space of the elements of displacement matrices combines translation with the rotation in such a way that the "distance" between two planar displacements is same as the metric used by Ravani and Roth [19]. In the context of four-bar mechanism synthesis, the method used by Ravani and Roth [19] solves the design problem of determining an image curve that passes through or near a set of given points. The image curve is algebraically given by intersection of two quadric hypersurfaces (constraint surfaces). The method is approximate in the sense that the constraint surfaces are approximated by their tangent hyperplane in the vicinity of the desired position. We now outline and conform Ravani and Roth [19]'s method for calculation of a new point in our problem:

Assuming that there exists an extreme point $\mathbf{m}^*$ at $u = u^*$ on the curve and a new point $\mathbf{m}$ is desired to be inserted to the initial set of given positions at the same parameter $u = u^*$, we define a normal error vector $\mathbf{e} = \mathbf{m} - \mathbf{m}^*$. The new point $\mathbf{m} = (m_1, m_2, m_3, m_4)$ should

satisfy the geometric constraints given by Eqs. (20), (21), and (22), rewritten as follows.

$$H_1(\mathbf{m}) : (m_3 - (\sigma - \tau)m_1 + (\sigma + \tau))^2 + (m_4 - (\sigma - \tau)m_2)^2 - r_1^2 = 0, \quad (25)$$
$$H_2(\mathbf{m}) : (m_3 + (\sigma - \tau)m_1 - (\sigma + \tau))^2 + (m_4 + (\sigma - \tau)m_2)^2 - r_2^2 = 0, \quad (26)$$
$$H_3(\mathbf{m}) : m_1^2 + m_2^2 - r_3^2 = 0, \quad (27)$$

where we have introduced new variables r_1, r_2, and r_3 that should satisfy following inequalities:

$$|a_1 - b_1| \le r_1 \le (a_1 + b_1), |a_2 - b_2| \le r_2 \le (a_2 + b_2),$$
$$|1.0 - \delta| \le r_3 \le (1.0 + \delta). \quad (28)$$

Equations (25), (26), and (27) describe three different quadric hypershells in the parameter space. We seek to minimize the square of the l^2 norm of the error vector $\mathbf{e}$ subject to the condition that $\mathbf{m}$ satisfies these inequalities. This optimization procedure yields the optimal values of variables r_1, r_2 and r_3, which in turn give the new point $\mathbf{m} = \mathbf{e}^* + \mathbf{m}^*$, where $\mathbf{e}^*$ is the optimized normal error vector. This new point $\mathbf{m}$ may not satisfy the kinematic constraints because the constraint surfaces are only approximated in this approach. In that case, this new point $\mathbf{m}$ is set as the new extreme point $\mathbf{m}^*$ and the process described above is repeated.

For faster computation of optimized normal error vector, Ravani and Roth [19] suggest an approximate method by using Taylor series expansion of the hypersurfaces (Eqs. (25) (26), and (27)) in the vicinity of the extreme point $\mathbf{m}^*$:

$$0 = H_1(\mathbf{m}^*) + \sum_{i=1}^4 \frac{\partial H_1(\mathbf{m}^*)}{\partial m_i} \Delta m_i,$$

$$0 = H_2(\mathbf{m}^*) + \sum_{i=1}^4 \frac{\partial H_2(\mathbf{m}^*)}{\partial m_i} \Delta m_i,$$

$$0 = H_3(\mathbf{m}^*) + \sum_{i=1}^2 2m_i^* \Delta m_i. \quad (29)$$

These equations can be assembled as follows:

$$\begin{bmatrix} \frac{\partial H_1}{\partial m_1} & \frac{\partial H_1}{\partial m_2} & \frac{\partial H_1}{\partial m_3} & \frac{\partial H_1}{\partial m_4} \\ \frac{\partial H_2}{\partial m_1} & \frac{\partial H_2}{\partial m_2} & \frac{\partial H_2}{\partial m_3} & \frac{\partial H_2}{\partial m_4} \\ 2m_1 & 2m_2 & 0 & 0 \end{bmatrix} \begin{bmatrix} \Delta m_1 \\ \Delta m_2 \\ \Delta m_3 \\ \Delta m_4 \end{bmatrix} = \begin{bmatrix} -H_1 \\ -H_2 \\ -H_3 \end{bmatrix}. \quad (30)$$

The above can also be written as

$$[J]\mathbf{e} = \mathbf{v}. \quad (31)$$

We solve for the normal error vector $\mathbf{e}$ by minimizing the Lagrangian function given as follows:

$$L(\mathbf{e}, \mathbf{a}) = \mathbf{e}^T[Q]\mathbf{e} + \mathbf{a}^T([J]\mathbf{e} - \mathbf{v}), \quad (32)$$

13th National Conference on Mechanisms and Machines (NaCoMM07),
IISc, Bangalore, India. December 12-13, 2007

NaCoMM-2007-102

where $\mathbf{a} = (a_1, a_2, a_3)$ is a vector of Lagrange multipliers, $\mathbf{e} = (m_1 - m_1^*, m_2 - m_2^*, m_3 - m_3^*, m_4 - m_4^*)$, $\mathbf{v} = (-H_1(\mathbf{m}^*), -H_2(\mathbf{m}^*), -H_3(\mathbf{m}^*))$,

and $[Q] = \begin{pmatrix} 1 & 0 & 0 & 0 \\ 0 & 1 & 0 & 0 \\ 0 & 0 & 1/4 & 0 \\ 0 & 0 & 0 & 1/4 \end{pmatrix}$.

Matrix $[Q]$ comes about from using a proper metric (as derived earlier) for the parameter space of the elements of the displacement matrix. Putting the condition for a minimum as

$$\frac{\partial L}{\partial e_i} = 0, i = 1, 2, 3, 4 \qquad (33)$$

where (e_1, e_2, e_3, e_4) are the coordinates of the vector $\mathbf{e}$ and assembling the solution equations, we obtain

$$2\mathbf{g} + [J]^T \mathbf{a} = 0, \qquad (34)$$

where $\mathbf{g} = (2e_1, 2e_2, e_3/2, e_4/2)$. If we transform the matrix $[J]$ to $[J']$ such that

$$[J'] = \begin{bmatrix} \dfrac{\partial H_1}{\partial m_1} & \dfrac{\partial H_1}{\partial m_2} & 4\dfrac{\partial H_1}{\partial m_3} & 4\dfrac{\partial H_1}{\partial m_4} \\ \dfrac{\partial H_2}{\partial m_1} & \dfrac{\partial H_2}{\partial m_2} & 4\dfrac{\partial H_2}{\partial m_3} & 4\dfrac{\partial H_2}{\partial m_4} \\ 2m_1 & 2m_2 & 0 & 0 \end{bmatrix}, \qquad (35)$$

then Eq. (34) changes to

$$2\mathbf{e} + [J']^T \mathbf{a} = 0. \qquad (36)$$

Thus, if $\mathbf{e}^*$ designates the solution to the error vector (or, the normal distance) then it should satisfy the equations

$$\begin{aligned} [J]\mathbf{e}^* &= \mathbf{v}, \\ 2\mathbf{e}^* + [J']^T \mathbf{a} &= 0. \end{aligned} \qquad (37)$$

Equation (37) gives an explicit formula for the solution error vector $\mathbf{e}^*$ as:

$$\mathbf{e}^* = [J']^T ([J][J']^T)^{-1} \mathbf{v}. \qquad (38)$$

Thus, we can determine the variables r_1, r_2, and r_3 by optimizing the function

$$E(\mathbf{m}, r_1, r_2, r_3) = (\mathbf{e}^*)^T \mathbf{e}^*, \qquad (39)$$

subject to constraints given by Eq. (28).
With normal error vector $\mathbf{e}^*$ known, the new point is given by

$$\mathbf{m} = \mathbf{e}^* + \mathbf{m}^*. \qquad (40)$$

Since the constraint surfaces have been approximated by their tangent hyperplanes in the vicinity of the extreme point $\mathbf{m}^*$, this new point $\mathbf{m}$ may not lie inside the constraint solids given by Eqs. (25), (26), and (27). If the new point does not satisfy the constraints, the newly obtained point $\mathbf{m}$ is set as an extreme point $\mathbf{m}^*$ and the procedure described above is repeated from Eq. (29)

until a new point $\mathbf{m}$ is obtained that satisfies the kinematic constraints. With this new point added to the set of initial positions, a new C^2 B-spline is generated that interpolates the points. If the new curve detects any further violation of the kinematic constraints, the optimization process is repeated until no further extreme points are found. This process at the end gives an interpolating motion that satisfies the kinematic constraints. Now, we present the algorithm:

Algorithm

1. Convert given positions of the coupler link into matrix elements $\mathbf{m}_i = (m_{i1}, m_{i2}, m_{i3}, m_{i4})$ using Eqs. (1) and (4) or, if given in terms of joint angles, by direct substitution into the homogeneous form of the displacement matrix.

2. Current list of points to be interpolated = given points $(\mathbf{m}_i; i = 1 \ldots n)$

3. Construct a C^2 cubic B-spline curve $\mathbf{m}(u)$ that interpolates $\mathbf{m}_i$ at parameter values u_i

4. Evaluate the extrema of $F_i(u); i = 1, 2, 3$ using Eq. (23). Repeat Steps (a) to (f) for all extrema.

   (a) Say, an extreme point is found at $u = u^*$.

   (b) Check if $\mathbf{m}(u^*)$ satisfies the kinematic constraints (Eqs. (25), (26), and (27)).

   (c) If yes, the curve is constrained; continue to Step 5. If no, designate $\mathbf{m}(u^*)$ as an extreme point $\mathbf{m}^*$ and continue.

   (d) Find a new point $\mathbf{m}$ (Eqs. (29) – (40)).

   (e) Check if the new point $\mathbf{m}$ satisfies kinematic constraints (Eqs. (25), (26), and (27)).

      i. If yes, continue to next Sub-step (f)

      ii. else, set $\mathbf{m}^* = \mathbf{m}$ and repeat from Sub-step (d).

   (f) Add $\mathbf{m}$ at $u = u^*$ to the current list of points to be interpolated and go to Step 3.

5. The parameter space curve $\mathbf{m}(u)$ defines a C^2 interpolating piecewise rational motion of degree 3 after substitution into Eq. (3).

We have observed that this algorithm always converges. In this algorithm, the B-spline curve is generated using a global interpolation scheme (Piegl and Tiller [2]). In this scheme, although moving one of the interpolating points changes the curve globally, the change in the curve diminishes away from the modification point.

4 Example

In this section, we present an example to demonstrate the algorithm presented earlier. Table 1 gives the elements of

13th National Conference on Mechanisms and Machines (NaCoMM07),
IISc, Bangalore, India. December 12-13, 2007

NaCoMM-2007-102

Table 1: **Elements of the displacement matrix of the given positions of the coupler link of a planar 6R closed chain**($a_1 = 1.0, b_1 = 3.0, a_2 = 4.0, b_2 = 3.2, g = 6.0, h = 3.6$)

i	$\mathbf{m}_i = (m_{i1}, m_{i2}, m_{i3}, m_{i4})$	u_i
1	$(1.0000, 0, 2.0449, -0.1941)$	0.0
2	$(0.8660, 0.5000, 1.9067, 1.5028)$	2.0
3	$(0.9659, -0.2588, -0.8893, 3.4851)$	5.0
4	$(0.9659, 0.2588, -0.7850, 3.2651)$	7.0
5	$(0.8568, 0.5157, -2.3005, 3.1447)$	10.0

Table 2: **Kinematic constraints of given planar 6R closed chain.** $\delta = 0.05$

i	Kinematic constraints (F_i)
1	$4.00 \le F_1 \le 16.00$
2	$0.64 \le F_2 \le 51.84$
3	$0.95 \le F_3 \le 1.05$

Figure 5: Unconstrained and constrained interpolation; kinematic constraint surface in a three-dimensional space parameterized by m_1, m_2, m_3 coordinates: all five extreme points ($\star$) violate circular constraint; algorithm adds five new points ($\square$).

Figure 6: Intersection of two constraint shells ($4.00 \le F_1 \le 16.00$ and $0.64 \le F_2 \le 51.84$) with $m_1 = 1$ hyperplane and the unconstrained and constrained curve: two extreme points with $F_1(8.83) = 2.77$ and $F_1(9.06) = 2.67$ violate the kinematic constraint: $4.00 \le F_1$

the displacement matrix $(m_{i1}, m_{i2}, m_{i3}, m_{i4})$ for five positions of the coupler link of a planar 6R closed chain along with their parameter values. The table also gives the link lengths and the distances between moving and the fixed pivots. The range of the inequality for the kinematic constraints given by Eqs. (20), (21), (22) are shown in Table 2.

For the input data given in the Table 1, our algorithm takes two iterations to produce a C^2 B-spline motion that satisfies all the kinematic constraints. In the first iteration, four extreme points are detected; out of which all the four violate the approximate rigid body constraint given by Eq. (22), and two of them also violate the constraint given by Eq. (20). In the second iteration, one extreme point is detected. This is shown partially in Fig. 5, where a part of the constraint surface parameterized by coordinates m_1, m_2, m_3 is shown. The figure shows the hypersurface given by Eq. (5), which is a cylinder perpendicular to $m_1 m_2$ plane. The initial unconstrained B-spline curve is shown by broken line and the initial positions to be interpolated are shown by round filled circles ('•') The extreme points detected in the first iteration are shown by the 'star' ('$\star$') symbol, while the lone extreme point detected in the second iteration is shown by a 'delta' ('$\triangle$') symbol. The figure also indicates the parameter and the value of the $F_i(u); i = 1, 3$ functions ((20), and (22)) at the extreme points. It can be clearly seen that none of the extreme points are on the hypercylinder, indicating a violation of rigid body constraint, however in this figure it is difficult to see the violation of the constraint given by Eq. (20). The algorithm adds five new points (indicated by '$\square$') corresponding to the five extreme points. The new curve lies on or very near (due to a choice of $\delta = 0.05$) to the hypercylinder and satisfies all the constraints. To visualize the violation of the other constraint, we show the intersection of the corresponding four dimensional constraint shells
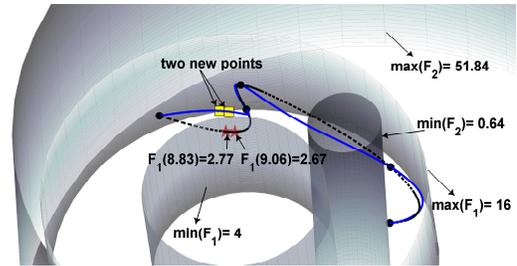
(Eqs.(20), (21)) with $m_1 = 1$ hyperplane in Fig. 6. In $m_1 = 1$ hyperplane, Eqs.(20) and (21) describe two elliptic cylindrical shells. The curve is constrained to lie inside the volume between the boundary surfaces. The figure shows two extreme points that violate the F_1 constraint (Eq.(20)). These two points are clearly seen to be outside the constraint shell bounded by surfaces marked as min(F_1) and max(F_1). These are the same two points, which violate the F_1 constraint in first iteration (see Fig. 5). Also shown are two new points ('$\square$') added by the algorithm and the constrained curve. The final interpolating curve satisfies all the constraints, which in the Cartesian space translates into a C^2 continuous B-spline rational motion of the planar 6R closed chain.

5 Rational Motions of Planar 4R and 5R Closed Chain

By transforming the equality relations of 4R and 5R closed chains from Eqs. (12) and (15) into inequalities, we can apply the same algorithm as presented before to do constrained interpolation for 4R and 5R closed chains as well. We have already seen how to transform the circular constraint into an inequality (Eq. (20)). Here we focus on the other equality constraints. We modify the equality constraints from

13th National Conference on Mechanisms and Machines (NaCoMM07),
IISc, Bangalore, India. December 12-13, 2007

NaCoMM-2007-102

Eq. (12) of planar 4R closed chains as follows:

$$(a_1 - \varepsilon_1)^2 \leq F_1(u) \leq (a_1 + \varepsilon_1)^2, \qquad (41)$$

$$(a_2 - \varepsilon_2)^2 \leq F_2(u) \leq (a_2 + \varepsilon_2)^2, \qquad (42)$$

where ε_1 and ε_2 are user-defined tolerances, and $F_1(u)$ and $F_2(u)$ have been previously defined. Thus, by choosing these tolerances to be as small as possible, the user can use the same algorithm to do constrained interpolation to a desired degree of satisfaction. The new points are added in the same way as described before. In case of planar 5R closed chain, we modify the only non-circular equality constraint in Eq. (15) to be same as the modified constraint given by Eq. (41).

6 Conclusions

In this paper, we presented a method for synthesizing piecewise rational motions subject to the kinematic constraints of the planar 6R closed chain by directly using the elements of the displacement matrix. This method has the advantage of being direct and produces lower degree motions. It was shown that the method is general enough to handle the planar 4R and 5R closed chains as well.

Acknowledgment

References

[1] Farin, G., 1996. *Curves and Surfaces for Computer-Aided Geometric Design: A Practical Guide*, 4th ed. Academic Press, New York.

[2] Piegl, L., and Tiller, W., 1995. *The Nurbs Book*. Springer, Berlin.

[3] Ravani, B., and Roth, B., 1984. "Mappings of spatial kinematics". *Journal of Mechanisms Transmissions and Automation in Design-Transactions of the ASME,* **106**(3), pp. 341–347.

[4] Ge, Q. J., and Ravani, B., 1994. "Computer-Aided Geometric Design Of Motion Interpolants". *ASME Journal of Mechanical Design,* **116**(3), pp. 756–762.

[5] Ge, Q. J., and Ravani, B., 1994. "Geometric Construction Of Bezier Motions". *ASME Journal of Mechanical Design,* **116**(3), pp. 749–755.

[6] Juttler, B., and Wagner, M. G., 1996. "Computer-Aided Design With Spatial Rational B-Spline Motions". *ASME Journal of Mechanical Design,* **118**(2), pp. 193–201.

[7] Wagner, M. G., 1994. "A Geometric Approach To Motion Design". Ph.d. dissertation, Technische Universitt Wien.

[8] Röschel, O., 1998. "Rational Motion Design - A Survey". *Computer-Aided Design,* **30**(3), pp. 169–178.

[9] Purwar, A., and Ge, Q. J., 2005. "On The Effect Of Dual Weights In Computer Aided Design Of Rational Motions". *ASME Journal of Mechanical Design,* **127**(5), pp. 967–972.

[10] Horsch, T., and Juttler, B., 1998. "Cartesian Spline Interpolation For Industrial Robots". *Computer-Aided Design,* **30**(3), pp. 217–224.

[11] Wagner, M., and Ravani, B., 1996. "Computer Aided Design Of Robot Trajectories Using Rational Motions". In *Recent Advances in Robot Kinematics*, J. Lenarcic and V. Parenti-Castelli, eds. Kluwer Academic Publishers, pp. 151–158.

[12] Jin, Z., and Ge, Q. J., 2007. "Computer Aided Synthesis Of Piecewise Rational Motion For Planar 2R and 3R Robot Arms". *ASME Journal of Mechanical Design,* **129**(10), pp. 1031–1036.

[13] Jin, Z., and Ge, Q. J., 2007. "Rational Motion Interpolation Under Kinematic Constraints Of Planar 6R Closed Chain". In ASME 2007 International Design Engineering Technical Conferences & Computers and Information in Engineering Conference, Paper No. DETC2006-99650, in press.

[14] Purwar, A., Zhe, J., and Ge, Q. J., 2006. "Computer Aided Synthesis Of Piecewise Rational Motions For Spherical 2R and 3R Robot Arms". In Proceedings of IDETC/CIE 2006 ASME 2006 International Design Engineering Technical Conferences, Paper No. DETC2006-99650.

[15] Purwar, A., Jin, Z., and Ge, Q. J., 2007. "Rational Motion Interpolation Under Kinematic Constraints Of Spherical 6R Closed Chains". *ASME Journal of Mechanical Design,* **accepted for publication**.

[16] Bottema, O., and Roth, B., 1979. *Theoretical Kinematics*. North Holland, Amsterdam.

[17] McCarthy, J. M., 1990. *Introduction to Theoretical Kinematics*. MIT.

[18] Jin, Z., and Ge, Q. J., 2007. "Constrained Motion Interpolation for Planar Open Kinematic Chains". *Mechanism and Machine Theory*(accepted for publication).

[19] Ravani, B., and Roth, B., 1983. "Motion Synthesis Using Kinematic Mappings". *Journal of Mechanisms Transmissions and Automation in Design-Transactions of the Asme,* **105**(3), pp. 460–467.

[20] Angeles, J., 2006. "Is there a characteristic length of a rigid-body displacement?". *Mechanism and Machine Theory,* **41**(8), pp. 884–896.